Biosensors and Bioelectronics 35 (2012) 507–511

Contents lists available at SciVerse ScienceDirect

Biosensors and Bioelectronics

journal homepage: www.elsevier.com/locate/bios

Short communication

DNA electrochemical biosensor based on thionine-graphene nanocomposite

Limei Zhu [a,b], Liqiang Luo [a,*], Zhenxin Wang [b,**]

[a] College of Sciences, Shanghai University, Shanghai 200444, PR China
[b] State Key Laboratory of Electroanalytical Chemistry, Changchun Institute of Applied Chemistry, Chinese Academy of Sciences, Changchun 130022, PR China

ARTICLE INFO

Article history:
Received 10 December 2011
Received in revised form 22 February 2012
Accepted 13 March 2012
Available online 22 March 2012

Keywords:
Graphene
Thionine
DNA electrochemical biosensor
Daunomycin

ABSTRACT

A novel protocol for development of DNA electrochemical biosensor based on thionine-graphene nanocomposite modified gold electrode was presented. The thionine-graphene nanocomposite layer with highly conductive property was characterized by scanning electron microscopy, transmission electron microscopy, cyclic voltammetry and electrochemical impedance spectroscopy. An amino-substituted oligonucleotide probe was covalently grafted onto the surface of the thionine-graphene nanocomposite by the cross-linker glutaraldehyde. The hybridization reaction on the modified electrode was monitored by differential pulse voltammetry analysis using an electroactive intercalator daunomycin as the indicator. Under optimum conditions, the proposed biosensor exhibited high sensitivity and low detection limit for detecting complementary oligonucleotide. The complementary oligonucleotide could be quantified in a wide range of 1.0×10^{-12} to 1.0×10^{-7} M with a good linearity ($R^2 = 0.9976$) and a low detection limit of 1.26×10^{-13} M (S/N = 3). In addition, the biosensor was highly selective to discriminate one-base or two-base mismatched sequences.

1. Introduction

The detection of specific DNA sequence is currently an area of tremendous interest since more and more research has proved that the mutations of genes are responsible for numerous inherited human disorders (Malley and Hutcheon, 2007; Van Borsel and Tetnowski, 2007; Chamcheu et al., 2011). Besides, pathogens responsible for disease states, bacteria and viruses, are also detectable *via* their unique nucleic acid sequences. Therefore, rapid and simple determination of specific sequences of DNA in human, viral and bacterial nucleic acids at low concentration is currently in great demand (Lucarelli et al., 2004). Many techniques including fluorescence (Yang et al., 2008; Liu et al., 2010a), electrochemiluminescence (Wei et al., 2007; Wang et al., 2010), electrochemistry (Chang et al., 2007; Liu et al., 2010b), surface plasmon resonance spectroscopy (Kick et al., 2010) and quartz crystal microbalance (Fei et al., 2011; Nie et al., 2007) have been developed for the DNA detection. In these bioassay systems, DNA electrochemical biosensors have attracted broad attention due to their advantages such as low cost, fast response, small size, good selectivity and miniaturization of instruments (Jiang et al., 2008; Riccardi et al., 2006; Peng et al., 2005; Yan et al., 2001).

Graphene, a two-dimensional sheet of sp^2 conjugated atomic carbon, has stimulated intense research interest because of its large specific surface area, high thermal and electrical conductivities (Novoselov et al., 2004; Kim et al., 2008), great mechanical strength (Zhao et al., 2010), and potential low manufacturing cost (Segal, 2009). Due to its excellent conductivity and electrocatalytic activity, graphene is an ideal material for the preparation of electrochemical sensors and biosensors (Shan et al., 2009; Zhou et al., 2009; Wang et al., 2009). Bonanni and Pumera (2011) developed a graphene platform to combine the sensitivity of electrochemical impedance spectroscopy (EIS) with the high selectivity of hairpin-shaped DNA probes for the rapid detection of single nucleotide polymorphism correlated to the development of Alzheimer's disease. Hu et al. (2011) constructed a novel gold nanoparticles-ionic liquid/3,4,9,10-perylene tetracarboxylic acid/graphene sensitive platform, which was successfully used for label-free impedance sensing of DNA. The graphene-based chemo/biosensors show a considerable prospect due to their good biocompatibility for biomolecules (Chen et al., 2008).

To expand the application of graphene, non-covalent functionalization between graphene sheets and aromatic organic molecules based on π-stacking interaction has been carried out (Su et al., 2009; Xu et al., 2008), which could preserve the intrinsic properties of graphene and improve its solubility (Ghosh et al., 2010). Thionine has a planar aromatic structure that allows strong interaction with the surface of graphene sheets through synergistic non-covalent charge-transfer and π–π stacking force (Chen et al., 2011). The positive charges on thionine facilitate the solubility and

* Corresponding author. Tel.: +86 21 66134734.
** Corresponding author. Tel.: +86 431 85262243.
E-mail addresses: luoliqw@yahoo.com.cn (L. Luo), wangzx@ciac.jl.cn (Z. Wang).

0956-5663/$ – see front matter © 2012 Elsevier B.V. All rights reserved.
doi:10.1016/j.bios.2012.03.026

prevent the aggregation of non-covalent functionalized graphene (Li et al., 2004). Moreover, due to a large amount of hydrophilic amino groups (—NH_2), thionine modified graphene sheets can covalently immobilize NH_2-substituted oligonucleotide probe by linker.

In this work, a DNA sensing platform based on thionine-graphene nanocomposite (Th-G) was developed. Using daunomycin as a hybridization indicator, the sensitive detection of complementary oligonucleotide was realized by monitoring differential pulse voltammetry (DPV) signal of daunomycin intercalated in double-stranded DNA (dsDNA). This sensing method provides potential applications for the ultrasensitive detection of different DNA sequences.

2. Experimental

2.1. Reagents

Graphite oxide (GO) was obtained from Nanjing XFNANO Materials Tech Co., Ltd., (Nanjing, China). Thionine, L-cysteine (Cys) and glutaraldehyde (GA, 25%) were provided by Sigma (USA). Daunomycin was purchased from Melone Pharmaceutical Co., Ltd., (Dalian, China). Hydrazine hydrate ($NH_2NH_2{\cdot}H_2O$, 80%) was purchased from Aladdin (Shanghai, China).

21-base synthetic oligonucleotide sequences related to anthrax lethal factor were provided by Sangon Biotech Co., Ltd., (Shanghai, China):

- Probe ssDNA (P_1): 5′-(NH_2-C_6) ATC AAT ATT TAA CAA TAA TCC-3′;
- Complementary ssDNA (C_1): 5′-GGA TTA TTG TTA AAT ATT GAT-3′;
- One mismatch-containing ssDNA (C_2): 5′-GGA TTA TTG TGA AAT ATT GAT-3′;
- Two mismatch-containing ssDNA (C_3): 5′-GGA TTA TGG TGA AAT ATT GAT-3′.

0.1 M phosphate buffer solution with 0.1 M KCl and 0.05 M NaCl (0.1 M PBS, pH 7.4) was used as the supporting electrolyte. All chemicals used in the experiments were of analytical grade. Milli-Q water (18.25 MΩ cm) was used throughout the experiments.

2.2. Instruments

Transmission electron microscopy (TEM) images were obtained by a Hitachi H-600 (Japan, at an acceleration voltage of 100 kV) and scanning electron microscopy (SEM) images were carried out on an XL30 ESEM-FEG (Netherlands, FEI Company, at an acceleration voltage of 15.0 kV).

Electrochemical measurements were performed using a CHI 660D electrochemical workstation (Shanghai CH Instrument Co., China). A conventional three-electrode system was used with a saturated calomel electrode (SCE) as the reference electrode, a platinum sheet as the counter electrode, and a modified gold electrode (AuE, 1.5 mm in diameter) as the working electrode. EIS measurements were tested by an Autolab PGSTST 30 analyzer (Metrohm Autolab B.V., Switzerland) using $[Fe(CN)_6]^{3-/4-}$ as the electrochemical probe. 5 mV amplitude of sine voltage signal was applied to the three-electrode system under open circuit potential, and the frequency varied from 0.1 Hz to 100 kHz.

2.3. Preparation of graphene and Th-G nanocomposite

Graphene was prepared according to the literature (Hummers and Offeman, 1958; Kovtyukhova et al., 1999). Briefly, the procedure was as following: the GO dispersion (5 mg dispersed in 50 mL water) was firstly exfoliated by sonicating under ambient conditions for 40 min. Then, $NH_2NH_2{\cdot}H_2O$ (1% v/v) was added into the GO dispersion. The resulting mixture was heated to 100 °C and kept stirring for 24 h. Subsequently, the solution was filtered, and the filtrate was discharged. Finally, black hydrophobic powder graphene was obtained by drying in vacuum at 60 °C, and stored at ambient conditions.

Th-G suspension was prepared as follows: 0.1 mg/mL of GO dispersion (5 mg of GO nanosheets into 50 mL water) was obtained by ultrasonication for 40 min at room temperature. After centrifugation at 3000 rpm for 5 min, the undissolved substance was discarded and the brown supernatant was kept for further use. Then, 10 mL of 2 mM of thionine aqueous was added into the above solution, and stirred vigorously for at least 12 h. After that, 200 μL $NH_2NH_2{\cdot}H_2O$ (80%) was dropped into the resulting dispersion. After being vigorously shaken for 10 min, the mixture was heated to 95 °C under reflux for 1 h. Finally, the stable dark dispersion was centrifuged and washed three times. The dark centrifugate was dissolved in 2 mL of distilled water.

2.4. Fabrication of DNA biosensors

The preparation of the DNA electrochemical biosensor is illustrated in Fig. 1. The bare AuE was carefully polished with 1.0, 0.3 and 0.05 μm alumina slurries, followed by successive sonication in Milli-Q water and ethanol for several minutes, respectively. Prior to use, the AuE was immersed in Piranha's solution for 10 min (a hot mixed solution of 30% H_2O_2 and concentrated H_2SO_4, volume ratio 3:7. Attention: strong hazardous chemicals), followed by rinsing with water and absolute ethanol. Then, the AuE was continuously scanned within a potential range of −0.35 V to +1.70 V in freshly prepared deoxygenated 0.5 M H_2SO_4 until a voltammogram characteristic of the cleaned AuE was established.

The freshly pretreated AuE was rinsed with water, dried with N_2 flow and then immersed in 20 mM Cys solution (0.1 M PBS, pH 7.4) for 24 h. A Cys-modified gold electrode (Cys/AuE) was obtained after thoroughly washing with water. The Cys/AuE was immersed into 0.5% GA solution for 2 h to obtain the GA modified gold electrode (GA/Cys/AuE). In this procedure, Cys was firstly self-assembled on the gold electrode, and then GA was covalently attached on the Cys/AuE. Then, 5 μL prepared Th-G suspension was dropped on the surface of the GA/Cys/AuE and dried in air to form Th-G nanocomposite modified electrode (Th-G/GA/Cys/AuE). The Th-G/GA/Cys/AuE was then washed with water and immersed into 0.5% GA solution for 2 h to obtain the GA modified electrode (GA/Th-G/GA/Cys/AuE). Finally, the GA/Th-G/GA/Cys/AuE was incubated in 20 μM P_1 for another 2 h to covalently immobilize the probe ssDNA, and thus the P_1/GA/Th-G/GA/Cys/AuE was obtained after washing with 0.1 M PBS (pH 7.4).

2.5. Hybridization and electrochemical measurements of the biosensor

The hybridization procedure was performed by immersing P_1/GA/Th-G/GA/Cys/AuE into 100 μL analyte solution (C_1, C_2 or C_3) with desired concentration for 40 min at 35 °C, and then the hybridized electrode was rinsed with 0.1 M PBS (pH 7.4) to remove the non-specifically adsorbed DNA. The obtained electrodes after hybridization with above different sequences were denoted as C_1-P_1/GA/Th-G/GA/Cys/AuE, C_2-P_1/GA/Th-G/GA/Cys/AuE and C_3-P_1/GA/Th-G/GA/Cys/AuE, respectively.

The hybridized electrode was placed in 10 μM daunomycin (0.1 M PBS, pH 7.4) for 15 min. The electrode was rinsed with 0.1 M PBS (pH 7.4) for several times to remove the physically adsorbed molecules. Then hybridized electrode was used for electrochemical measurements.

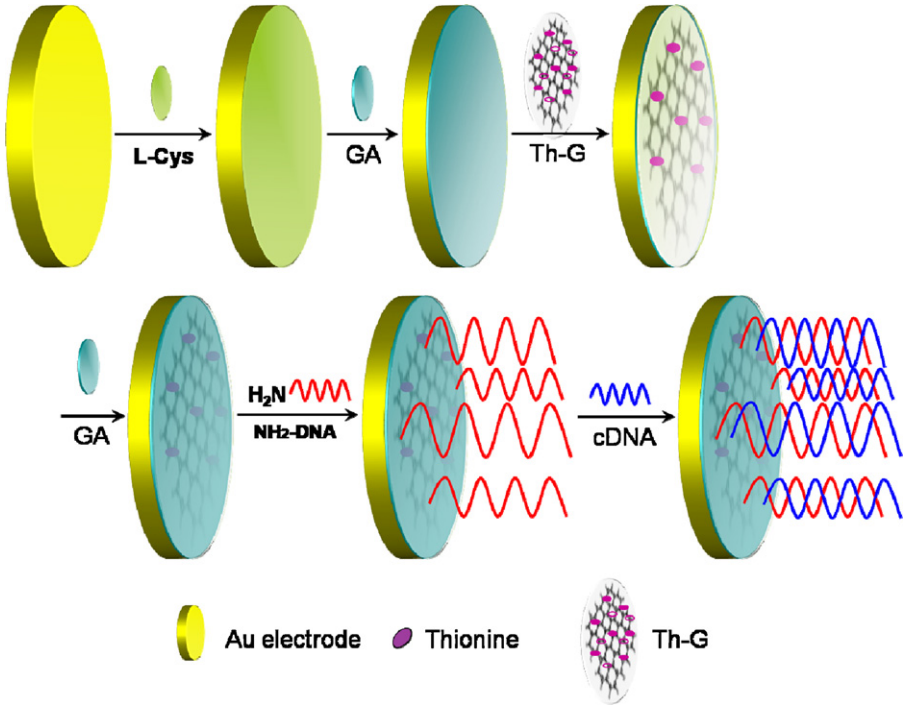

Fig. 1. Schematic diagram of covalent immobilization of NH_2-substituted probe ssDNA on Th-G nanocomposite using glutaraldehyde as an arm linker.

3. Results and discussion

3.1. Characterization of the graphene and Th-G nanocomposite

The morphology of the prepared graphene and Th-G nanocomposite characterized with SEM and TEM was shown in Fig. S1 (Supplementary information). Fig. S1A reveals the typical crumpled and wrinkled graphene sheet structure on the surface of the glassy carbon substrate. TEM image of graphene (Fig. S1B, Supplementary information) shows that graphene sheets were difficult to be dispersed in aqueous solution and always reunited with high-density large aggregates. As can be seen from the SEM image of Th-G nanocomposite (Fig. S1C, Supplementary information), a large amount of thionine molecules were attached to the graphene sheets. From the TEM image in Fig. S1D, unlike graphene sheets, the graphene modified by thionine became well-exfoliated and its solubility in water was improved after the interaction with thionine molecules. The results can be attributed to the thionine molecules attached onto the individual graphene sheets making graphene surface more hydrophilic.

UV–vis absorption spectrum was performed to study the π–π interaction between thionine and graphene. Fig. S2 (See Supplementary information) illustrates the absorption spectra of thionine solution, graphene oxide, graphene and Th-G suspension. The spectrum obtained from the graphene oxide dispersion (curve b) exhibits a strong absorption band at 230 nm attributing to π–π^* transitions of aromatic C=C bonds. The absorption band red-shifted to 275 nm, when graphene oxide was reduced to graphene (curve c), indicating the restoration of a π-conjugation network. The spectrum of thionine appears two characteristic adsorption peaks. One is located in near-ultraviolet region around 283 nm, while the other is located in visible region around 600 nm, which correspond to the π–π^* transitions of aromatic rings and the n–π^* transitions of C=N bond, respectively. The two corresponding absorption peaks can also be observed from the spectrum of Th-G, indicating the presence of thionine molecules on graphene. The red-shift for the absorption peak at 630 nm and blue-shift for the other absorption peak at 280 nm provide further evidence on the interaction between graphene and thionine molecules (Li et al., 2004; Chen et al., 2011; Wei et al., 2010).

3.2. Electrochemical characterization of different electrodes

The properties of different electrodes were examined by EIS exploiting the solution-based redox probe $[Fe(CN)_6]^{3-/4-}$, and the results were shown in Fig. S3 (See Supplementary information). In EIS, the semicircle portion observed at high frequencies corresponds to the electron transfer limiting process. When Cys was assembled onto AuE surface, the R_{ct} value (48 Ω, curve b) decreased compared with that of the bare AuE (351 Ω, curve a), suggesting that positive charges of the amino groups electrostatically favored the diffusion of negatively charged ferrocyanide molecules to the electrode surface and Cys acted as a so-called promoter in the electron transfer procedure (Tian et al., 2002; Liu et al., 2006). However, the R_{ct} value of GA/Cys/AuE (1063 Ω, curve c) is greatly increased, indicating that GA acted as an insulating layer which made the interfacial electron transfer difficult. After Th-G and GA being modified on AuE (curve d and curve e), the AC impedance spectra of the Th-G/GA/Cys/AuE and GA/Th-G/GA/Cys/AuE showed lower interfacial R_{ct} (20 Ω and 41 Ω, respectively), indicating that the Th-G layer improved the electron transfer process on the electrode surface. This is because that many small band gaps on Th-G are favorable for conducting electrons (Stankovich et al., 2006; Noll et al., 1998). After being treated with P_1 and C_1, P_1/GA/Th-G/GA/Cys/AuE and C_1-P_1/GA/Th-G/GA/Cys/AuE showed obviously different impedance curves f and g from the curves a–e (the corresponding R_{ct} increased to 349 Ω and 660 Ω, respectively). The increased R_{ct} can be ascribed to negative charges of DNA immobilized on the electrodes which are against the diffusion of negatively charged ferrocyanide molecules to the electrode surface. In order to verify EIS results, cyclic voltammograms (CVs) of different

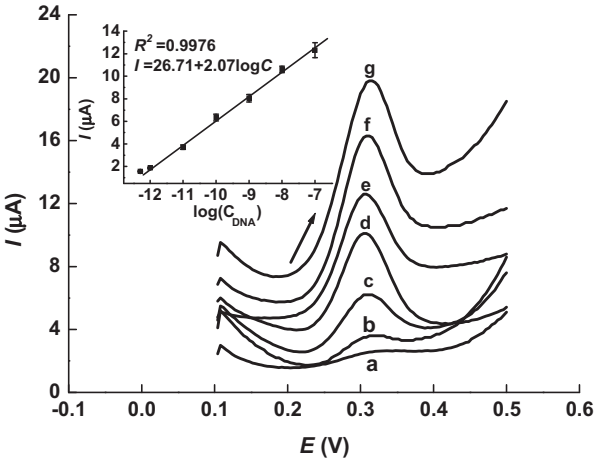

Fig. 2. DPV of P_1/GA/Th-G/GA/Cys/AuE without daunomycin (a), C_1-P_1/GA/Th-G/GA/Cys/AuE varying the concentration of C_1 from 1.0×10^{-12} M (b), 1.0×10^{-11} M (c), 1.0×10^{-10} M (d), 1.0×10^{-9} M (e), 1.0×10^{-8} M (f) and 1.0×10^{-7} M (g) in 0.1 M PBS (pH 7.4), intercalating with 10 μM daunomycin for 15 min; inset: the calibration curve of the biosensor.

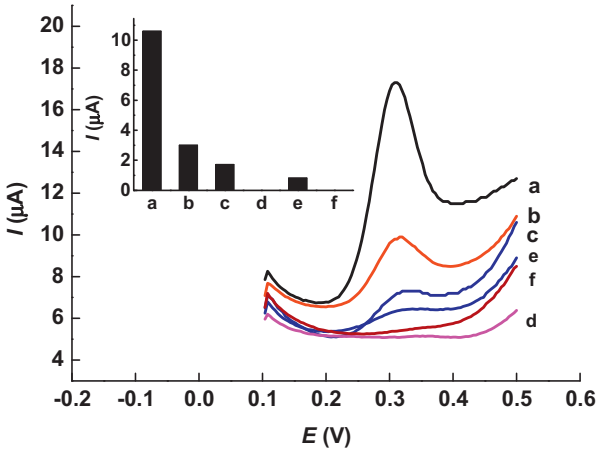

Fig. 3. DPV of C_1-P_1/GA/Th-G/GA/Cys/AuE (a), C_2-P_1/GA/Th-G/GA/Cys/AuE (b), C_3-P_1/GA/Th-G/GA/Cys/AuE (c) and P_1/GA/Th-G/GA/Cys/AuE (e) in 0.1 M PBS (pH 7.4), intercalating with 10 μM daunomycin for 15 min; DPV of P_1/GA/Th-G/GA/Cys/AuE (d) and C_1-P_1/GA/Th-G/GA/Cys/AuE (f) in 0.1 M PBS (pH 7.4), without intercalating with 10 μM daunomycin. The concentration of C_1–C_3 was 1.0×10^{-8} M.

modified electrodes in 5 mM $[Fe(CN)_6]^{3-/4-}$ solution are presented in Fig. S4 (See Supplementary information).

CVs of different modified electrodes after Th-G immobilization were recorded from −0.70 V to 0.20 V in 0.1 M PBS (pH 7.4), as shown in Fig. S5 (See Supplementary information). When Th-G was immobilized onto the surface of modified electrode, a couple of well-defined and diffusion-limited redox peaks were obtained. This is in accordance with literature (Tang et al., 2006), revealing that the thionine attached on graphene retained the redox properties. When P_1 was covalently attached onto the electrode through cross-linker, an obvious decrease of the redox peak current of thionine is observed. Under this immobilized conditions, we found that the surface loading of ssDNA is approximately 1.5×10^{13} molecules cm^{-2}, which is higher than that of literature reported (Ricci et al., 2007). After 1.0×10^{-8} M C_1 was captured, further current decrease appears, indicating that dsDNA formed an electron-transfer and mass-transfer blocking layer, which greatly inhibited the reaction on the electrode surface. The graphene modified surface also reveals high hybridization capacity; for instance, the hybridization efficiency of immobilized P_1 can reach 50%, when the hybridization is performed with a solution containing 1.0×10^{-8} M C_1.

3.3. Oligonucleotides detection with the proposed sensor

DPV, a highly sensitive electrochemical technique, was used for the detection of oligonucleotides. DPV measurements were conducted from +0.10 V to +0.50 V with the pulse amplitude 50 mV in 0.1 M PBS (pH 7.4). Under this condition, a peak related to the oxidation of daunomycin was obtained at around +0.31 V and taken as the electrochemical measurement signal.

Factors affecting the hybridization were optimized. The experimental results show that the best hybridized temperature, hybridized time and intercalation time of daunomycin were 35 °C, 40 min and 15 min for this system, respectively (See Fig. S7 in the Supplementary information).

Under optimal conditions, the analytical performance of the DNA biosensor was tested using the P_1/GA/Th-G/GA/Cys/AuE to hybridize with C_1 of different concentrations. Fig. 2 shows representative DPV curves of the oxidation of daunomycin at the C_1-P_1/GA/Th-G/GA/Cys/AuE. It can be observed that the peak current of daunomycin increased with the C_1 concentration increasing. The increase of peak current is linear with the C_1 concentration in the range from 1.0×10^{-12} M to 1.0×10^{-7} M (see the inset of Fig. 2). The regression equation is I (μA) = 26.71 + 2.07 log C (M) and the correlation coefficient is R^2 = 0.9976. The limit of detection is 1.26×10^{-13} M (S/N = 3). The performance of the proposed sensor was better than or comparable to that of other nanomaterials modified electrodes (See Table S1 in the Supplementary information).

3.4. The selectivity of the DNA sensor

Selectivity is a crucial factor to evaluate the performance of a DNA biosensor. In this work, the selectivity was explored using the P_1/GA/Th-G/GA/Cys/AuE to hybridize with different sorts of DNA sequences. Fig. 3 displays the comparison of DPV signals obtained from P_1/GA/Th-G/GA/Cys/AuE hybridized with C_1, C_2 and C_3, respectively. As can be seen from Fig. 3, no current response can be observed at the C_1-P_1/GA/Th-G/GA/Cys/AuE without intercalating with daunomycin (column f). However, after intercalating with 10 μM daunomycin, the response current at C_1-P_1/GA/Th-G/GA/Cys/AuE was greatly enhanced, demonstrating a sensitive detection of C_1 (column a). For one and two-base mismatched ssDNA, the C_2-P_1/GA/Th-G/GA/Cys/AuE and C_3-P_1/GA/Th-G/GA/Cys/AuE show smaller responses, respectively (column b and c). It can be seen that very small current responses appear at the P_1/GA/Th-G/GA/Cys/AuE with or without intercalating with daunomycin (column e and d), indicating that the presence of non-specific adsorption of daunomycin will not influence the response of the electrode. These results show that the DNA sensor performed good selectivity.

3.5. Reproducibility and stability of the DNA sensor

To characterize the reproducibility, the DNA sensor was tested in 0.1 M PBS (pH 7.4). Five parallelly prepared P_1/GA/Th-G/GA/Cys/AuEs were performed and then hybridized with 1.0×10^{-8} M C_1, respectively. An acceptable relative standard deviation (R.S.D.) of 8.3% (n = 5) for the current value of DPV was estimated, which shows the high reproducibility of the DNA detection. When stored in 0.1 M PBS (pH 7.4) at 4 °C for more than two weeks, the current response for the sensor decreased quickly (about 71% of its initial value) in the first five days, and then maintained stable from 5 to 14 days, demonstrating that the proposed DNA biosensor has good stability. (See Fig. S8 in the Supplementary information).

4. Conclusion

The successful preparation of the DNA electrochemical biosensor demonstrated the strong covalent immobilization of probe ssDNA to the surface of Th-G/GA/Cys/AuE *via* GA linker. Due to the large specific area and good conductivity of the graphene, thionine modified graphene provide a promising platform with high sensitivity and advantageous detection limit of DNA analysis. In a word, this work establishes a methodology for the developing of DNA biosensors with good analytical properties.

Acknowledgments

The authors would like to thank the National Science Foundation of China (no. 20875087, 20975066, 61171033), National Basic Research Program of China (no. 2011CB935800) for financial supports, and Leading Academic Discipline Project of Shanghai Municipal Education Commission (J50102).

Appendix A. Supplementary data

Supplementary data associated with this article can be found, in the online version, at doi:10.1016/j.bios.2012.03.026.

References

Bonanni, A., Pumera, M., 2011. ACS Nano 5, 2356–2361.
Chamcheu, J.C., Siddiqui, I.A., Syed, D.N., Adhami, V.M., Liovic, M., Mukhtar, H., 2011. Archives of Biochemistry and Biophysics 508, 123–137.
Chang, H.X., Yuan, Y., Shi, N.L., Guan, Y.F., 2007. Analytical Chemistry 79, 5111–5115.
Chen, C., Zhai, W.T., Lu, D.D., Zhang, H.B., Zheng, W.G., 2011. Materials Research Bulletin 46, 583–587.
Chen, H.Q., Muller, M.B., Gilmore, K.J., Wallace, G.G., Li, D., 2008. Advanced Materials 20, 3557–3561.
Fei, Y.H., Jin, X.Y., Wu, Z.S., Zhang, S.B., Shen, G.L., Yu, R.Q., 2011. Analytica Chimica Acta 691, 95–102.
Ghosh, A., Rao, K.V., George, S.J., Rao, C.N.R., 2010. Chemistry: A European Journal 16, 2700–2704.
Hu, Y.W., Hua, S.C., Li, F.H., Jiang, Y.Y., Bai, X.X., Li, D., Niu, L., 2011. Biosensors and Bioelectronics 26, 4355–4361.
Hummers, S.W., Offeman, R.E., 1958. Journal of the American Chemical Society 80, 1339.
Jiang, C., Yang, T., Jiao, K., Gao, H.W., 2008. Electrochimica Acta 53, 2917–2924.
Kick, A., Bönsch, M., Katzschner, B., Voigt, J., Herr, A., Brabetz, W., Jung, M., Sonntag, F., Klotzbach, U., Danz, N., Howitz, S., Mertig, M., 2010. Biosensors and Bioelectronics 26, 1543–1547.
Kim, K., Park, H.J., Woo, B.-C., Kim, K.J., Kim, G.T., Yun, W.S., 2008. Nano Letters 8, 3092–3096.
Kovtyukhova, N.I., Ollivier, P.J., Martin, B.R., Mallouk, T.E., Chizhik, S.A., Buzaneva, E.V., Gorchinskiy, A.D., 1999. Chemistry of Materials 11, 771–778.
Li, Q.W., Zhang, J., Yan, H., He, M.S., Liu, Z.F., 2004. Carbon 42, 287–291.
Liu, F., Choi, J.Y., Seo, T.S., 2010a. Biosensors and Bioelectronics 25, 2361–2365.
Liu, S.F., Liu, J., Han, X.P., Cui, Y.N., Wang, W., 2010b. Biosensors and Bioelectronics 25, 1640–1645.
Liu, Y., Yuan, R., Chai, Y.Q., Tang, D.P., Dai, J.Y., Zhong, X., 2006. Sensors and Actuators B 115, 109–115.
Lucarelli, F., Marrazza, G., Turner, A.P.F., Mascini, M., 2004. Biosensors and Bioelectronics 19, 515–530.
Malley, M.O., Hutcheon, R.G., 2007. Journal of the American Medical Directors Association 8, 332–334.
Nie, L.B., Yang, Y., Li, S., He, N.Y., 2007. Nanotechnology 18, 305501–305505.
Noll, J.D., Nicholson, M.A., Vanpatten, P.G., Chung, C.W., Murick, M.L., 1998. Journal of the Electrochemical Society 145, 3320–3328.
Novoselov, K.S., Geim, A.K., Morozov, S.V., Jiang, D., Zhang, Y., Dubonos, S.V., Grigorieva, I.V., Firsov, A.A., 2004. Science 306, 666–669.
Peng, H., Soeller, C., Vigar, N., Kilmartin, P.A., Cannell, M.B., Bowmaker, G.A., Cooney, R.P., Travas-Sejdic, J., 2005. Biosensors and Bioelectronics 20, 1821–1828.
Riccardi, C.S., Yamanaka, H., Josowicz, M., Kowalik, J., Mizaikoff, B., Kranz, C., 2006. Analytical Chemistry 78, 1139–1145.
Ricci, F., Lai, R.Y., Plaxco, K.W., 2007. Chemical Communications 36, 3768–3770.
Segal, M., 2009. Nature Nanotechnology 4, 612–614.
Shan, C., Yang, H., Song, J., Han, D., Ivaska, A., Niu, L., 2009. Analytical Chemistry 81, 2378–2382.
Stankovich, S., Dikin, D.A., Dommett, G.H.B., Kohlhaas, K.M., Zimney, E.J., Stach, E.A., Piner, R.D., Nguyen, S.T., Ruoff, R.S., 2006. Nature 442, 282–286.
Su, Q., Pang, S.P., Alijani, V., Li, C., Feng, X.L., Müllen, K., 2009. Advanced Materials 21, 3191–3195.
Tang, D.P., Yuan, R., Chai, Y.Q., 2006. Electroanalysis 18, 259–266.
Tian, Y., Shioda, M., Kasahara, S., Okajima, T., Mao, L., Hisabori, T., Ohsaka, T., 2002. Biochimica et Biophysica Acta 1569, 151–158.
Van Borsel, J., Tetnowski, J.A., 2007. Journal of Fluency Disorders 32, 279–296.
Wang, X.Y., He, P.G., Fang, Y.Z., 2010. Journal of Luminescence 130, 1481–1484.
Wang, Y., Li, Y.M., Tang, L.H., Lu, J., Li, J.H., 2009. Electrochemistry Communications 11, 889–892.
Wei, H., Du, Y., Kang, J.Z., Wang, E.K., 2007. Electrochemistry Communications 9, 1474–1479.
Wei, Q., Mao, K.X., Wu, D., Dai, Y.X., Yang, J., Du, B., Yang, M.H., Li, H., 2010. Sensors and Actuators B 149, 314–318.
Xu, Y.X., Bai, H., Lu, G.W., Li, C., Shi, G.Q., 2008. Journal of the American Chemical Society 130, 5856–5857.
Yan, F., Erdem, A., Meric, B., Kerman, K., Ozsoz, M., Sadik, O.A., 2001. Electrochemistry Communications 3, 224–228.
Yang, R., Jin, J., Chen, Y., Shao, N., Kang, H., Xiao, Z., Tang, Z., Wu, Y., Zhu, Z., Tan, W., 2008. Journal of the American Chemical Society 130, 8351–8358.
Zhao, X., Zhang, Q.H., Chen, D.J., 2010. Macromolecules 43, 2357–2363.
Zhou, M., Zhai, Y.M., Dong, S.J., 2009. Analytical Chemistry 81, 5603–5613.